Clinical Population Pharmacokinetics and Toxicodynamics of Linezolid

Lauren M. Boak,[a]* Craig R. Rayner,[a,b] M. Lindsay Grayson,[c,d] David L. Paterson,[e]* Denis Spelman,[f] Sharmila Khumra,[c,h] Blair Capitano,[e]* Alan Forrest,[g] Jian Li,[a] Roger L. Nation,[a] Jurgen B. Bulitta[a,g,h]

Drug Delivery, Disposition and Dynamics, Monash Institute of Pharmaceutical Sciences, Monash University (Parkville campus), Parkville, Australia[a]; d3 Medicine LLC, Parsippany, New Jersey, USA[b]; Department of Medicine, Austin Hospital, Melbourne, Australia[c]; Department of Epidemiology and Preventive Medicine, Monash University, Melbourne, Australia[d]; University of Pittsburgh Medical Center, Pittsburgh, Pennsylvania, USA[e]; Department of Infectious Diseases, Alfred Hospital and Monash University, Melbourne, Australia[f]; School of Pharmacy and Pharmaceutical Sciences, SUNY at Buffalo, Buffalo, New York, USA[g]; Centre for Medicine Use and Safety, Monash University (Parkville campus), Parkville, Australia[h]

Thrombocytopenia is a common side effect of linezolid, an oxazolidinone antibiotic often used to treat multidrug-resistant Gram-positive bacterial infections. Various risk factors have been suggested, including linezolid dose and duration of therapy, baseline platelet counts, and renal dysfunction; still, the mechanisms behind this potentially treatment-limiting toxicity are largely unknown. A clinical study was conducted to investigate the relationship between linezolid pharmacokinetics and toxicodynamics and inform strategies to prevent and manage linezolid-associated toxicity. Forty-one patients received 42 separate treatment courses of linezolid (600 mg every 12 h). A new mechanism-based, population pharmacokinetic/toxicodynamic model was developed to describe the time course of plasma linezolid concentrations and platelets. A linezolid concentration of 8.06 mg/ liter (101% between-patient variability) inhibited the synthesis of platelet precursor cells by 50%. Simulations predicted treatment durations of 5 and 7 days to carry a substantially lower risk than 10- to 28-day therapy for platelet nadirs of $<100 \times 10^9/$ liter. The risk for toxicity did not differ noticeably between 14 and 28 days of therapy and was significantly higher for patients with lower baseline platelet counts. Due to the increased risk of toxicity after longer durations of linezolid therapy and large between-patient variability, close monitoring of patients for development of toxicity is important. Dose individualization based on plasma linezolid concentration profiles and platelet counts should be considered to minimize linezolid-associated thrombocytopenia. Overall, oxazolidinone therapy over 5 to 7 days even at relatively high doses was predicted to be as safe as 10-day therapy of 600 mg linezolid every 12 h.

The oxazolidinone linezolid remains an important antimicrobial agent against multidrug-resistant Gram-positive pathogens. Linezolid was originally approved for up to a 28-day duration of therapy to treat indicated infections, such as skin and skin structure infections, community-acquired and nosocomial pneumonia, and vancomycin-resistant *Enterococcus faecium* (1). Still, linezolid has been and continues to be used for longer treatment durations (2), an approach facilitated by favorable pharmacokinetic (PK) properties, such as close to 100% oral bioavailability (3, 4). Linezolid treatment is associated with reversible thrombocytopenia, particularly when used for ≥14 days (2, 5–7). Patients with baseline platelet counts of 241 × 10⁹/liter or less (8) and renal insufficiency (9) are at particular risk for linezolid-induced thrombocytopenia. In this context, implementing systematic monitoring programs (10) and predicting and minimizing the extent of platelet decline in high-risk patients is important.

Evidence for a relationship between linezolid exposure and thrombocytopenia exists. Data from highly debilitated, critically ill compassionate-use patients were used to develop a model relating changes in platelet counts to linezolid exposure, treatment duration, and baseline platelet counts (11). A population model has recently been developed based on data obtained in 45 Japanese patients to quantitatively describe the relationship between linezolid exposure and platelet counts (12). In the present paper, we greatly extended the exposure-response relationship established by Forrest et al. (11) and performed an in-depth mechanism-based modeling analysis of the time course and potential mechanisms of the toxicodynamics of linezolid. This allowed us to pre-

dict the time course of platelet counts for linezolid dosage regimens with different dose levels, durations of therapy, and changes in dose intensity over time.

The mechanism(s) responsible for linezolid-induced thrombocytopenia have not been clearly delineated. Classical myelosuppression has been implicated, in which direct toxicity to bone marrow or hematopoietic cells is observed (13). Some case reports support a drug-induced immune-mediated mechanism, based on observations that include the presence of megakaryocytes or drug-related antiplatelet antibodies and the abrupt onset of platelet decline following initiation of linezolid therapy (14, 15). Sasaki et al. depicted linezolid-induced thrombocytopenia in their model as the inhibition of the proliferation of progenitor cells (12).

The current study aimed to characterize the relationship between linezolid concentrations and thrombocytopenia over time
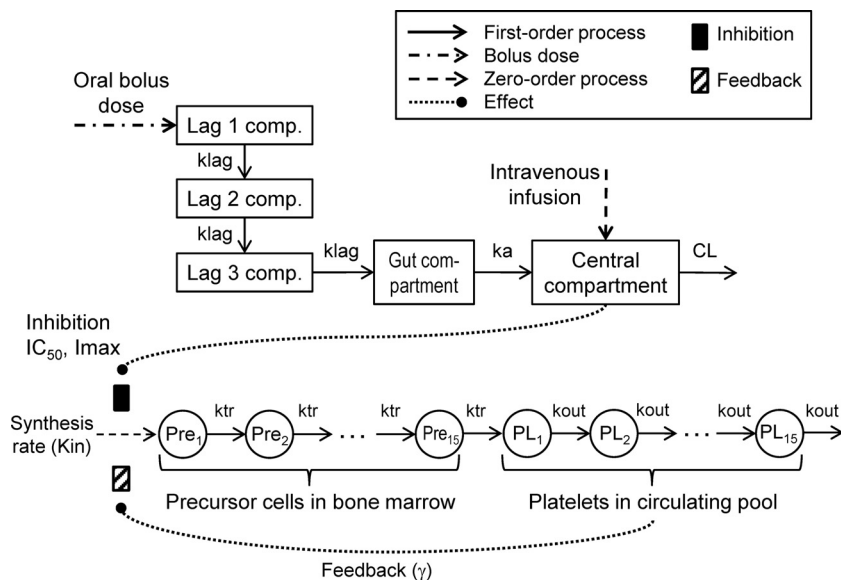
FIG 1 Structure of the final mechanism-based population pharmacokinetic/toxicodynamic model. The pharmacokinetic model is comprised of three absorption lag compartments, a gut compartment, and a central compartment. One series of 15 transit compartments was used to describe platelet precursor cells in the bone marrow, and another series of 15 transit compartments to describe platelets in the circulating pool. Platelets displayed a feedback effect on the synthesis of platelet precursor cells. A lack of platelets in the circulating pool compared to the platelet count at steady state caused a stimulation of platelet precursor synthesis, and an excess of platelets in the circulating pool caused an inhibition of platelet precursor synthesis.

and to predict the time course and extent of toxicity for standard and innovative linezolid dosage regimens. These analyses helped guide strategies to predict and manage this toxicity. We utilized mechanism-based population pharmacokinetic/toxicodynamic (PK/TD) modeling and explored risk factors for the development of linezolid-induced thrombocytopenia.

(These data were presented in part at the 46th Interscience Conference on Antimicrobial Agents and Chemotherapy, San Francisco, CA, 27 to 30 September 2006.)

MATERIALS AND METHODS

Design and patient population. This study was a prospective, open-labeled, observational study of patients receiving linezolid treatment at three hospitals: the Departments of Infectious Diseases at the Alfred and Austin Hospitals, Melbourne, Victoria, Australia, and the Transplant Unit of the University of Pittsburgh Medical Center (UPMC), Pittsburgh, PA, USA. The study protocol was approved by the relevant ethics committees/institutional review boards at the hospitals and Monash University and was carried out in accordance with the revised version of the Declaration of Helsinki.

Patients were enrolled within the 28-month period between October 2004 and January 2007. Males or nonpregnant females of at least 18 years of age initiated on linezolid therapy by their treating physician were included in the study. Patient medical history, demographic data, previous and concomitant medication, and linezolid dosage details were collected. Hematological parameters (including platelet and hemoglobin values) were measured up to 5 days before the start of linezolid therapy and collected at least weekly during treatment. Details on potential contributors to thrombocytopenia (e.g., preexisting conditions, concomitant drugs, bleeding events, and blood products) were collected before and during linezolid therapy.

Drug administration and PK sample collection. Patients received 600 mg intravenous or oral linezolid twice daily for at least 4 days; some patients received both intravenous and oral therapy but not simultaneously. Blood samples were drawn at time points in relation to one linezolid dose (predose and 2, 4, and 8 h postdose) in all but one patient,

whose samples were collected around two consecutive linezolid doses to generate peak and trough concentrations. Where possible, the PK samples were collected within the first week of therapy to precede any drug-induced hematological toxicity. Blood samples were drawn into 10 ml K_3EDTA Vacutainer tubes (Becton, Dickinson, Franklin Lakes, NJ, USA) and centrifuged to harvest plasma for immediate freezing and storage at −20°C. Plasma linezolid concentrations were measured using a validated high-performance liquid chromatography (HPLC) method [16].

Population pharmacokinetic model structure. Pharmacokinetic models with one or two disposition compartments and first-order absorption were evaluated. To describe an absorption delay, models with or without up to 10 serial absorption-lag compartments were assessed. Elimination was described by a first-order (linear), mixed-order (Michaelis-Menten), or parallel first-order and mixed-order process. Additionally, an inhibition compartment approach was considered to describe a time-dependent saturation of linezolid clearance [17–19]. Oral bioavailability was initially estimated and eventually fixed at 100% [4].

The differential equations used to describe the amount of drug in the absorption lag compartments (Fig. 1, Lag 1, Lag 2, and Lag 3), gut compartment, and central compartment (A1) were as follows (initial condition [IC] for all, 0):

$$\frac{d\text{Lag1}}{dt} = -k_{\text{lag}} \cdot \text{Lag1} \tag{1}$$

$$\frac{d\text{Lag2}}{dt} = k_{\text{lag}} \cdot \left(\text{Lag1} - \text{Lag2}\right) \tag{2}$$

$$\frac{d\text{Lag3}}{dt} = k_{\text{lag}} \cdot \left(\text{Lag2} - \text{Lag3}\right) \tag{3}$$

$$\frac{d\text{Gut}}{dt} = k_{\text{lag}} \cdot \text{Lag3} - k_a \cdot \text{Gut} \tag{4}$$

$$\frac{d\text{A1}}{dt} = k_a \cdot \text{Gut} + R_{\text{Infusion}} - \text{CL} \cdot C_1 \tag{5}$$

The k_{lag} is the rate constant describing the absorption lag phase, k_a is

the absorption rate constant, R_{Infusion} is the rate of infusion, C_1 is the drug concentration in the central compartment, and CL is total clearance.

The area under the plasma concentration-time curve over 24 h (AUC_{24}), averaged over days 1 to 7 of treatment, was calculated by numerical integration of the individually fitted concentration profiles. For patients receiving linezolid for less than 7 days, the average AUC_{24} was calculated over the reduced treatment period. The average AUC_{24} was used because dosing times changed slightly during therapy in some patients.

Mechanism-based population pharmacokinetic/toxicodynamic model. The effect of linezolid treatment on platelet counts was examined. A transit compartment approach (20) was employed to describe the life span of platelet precursor cells and platelets. Turnover models with 1, 3, 6, 9, 12, or 15 compartments each for platelet precursor cells (Pre_1 to Pre_{15}) and platelets (PL_1 to PL_{15}) were considered to describe different profiles of the life span distribution for platelets (21–23). The existence of a larger number of compartments for a specific cell type results in a narrower distribution of platelet life spans for a given patient.

Different possible mechanisms of linezolid-induced thrombocytopenia have been described (13–15). In the current investigation, linezolid was assumed to inhibit the synthesis of platelet precursor cells (mechanism 1 [Fig. 1]), kill platelet precursor cells (mechanism 2), kill platelets (mechanism 3), or stimulate the natural loss rate constant of platelets (k_{out}) (mechanism 4). Mechanism 2 involved linezolid stimulating a loss of platelet precursor cells from compartments Pre_1 to Pre_{15}, and mechanism 3 a loss of platelets from compartments PL_1 to PL_{15} (Fig. 1). Mechanisms 2 and 3 could be explained by an immune-mediated elimination (14) and were implemented using a saturable, Hill-type loss function.

Based on the results from Sasaki et al. (12) a homeostatic feedback mechanism was implemented, contributing to a temporary increase in platelet counts above the baseline after cessation of linezolid therapy. Our models considered that a decline of platelets below the patient-specific platelet baseline either stimulated the synthesis (K_{in}) of platelet precursors or enhanced the transfer rate constant (k_{tr}) of platelet precursors. The latter process was assumed to result in a shorter maturation time of platelet precursor cells.

For the model with mechanism 1, the decline of platelet counts was modeled through inhibition of platelet precursor synthesis by linezolid (Fig. 1). The inhibitory function incorporated parameters for the maximal extent of inhibition (I_{max}) and the concentration achieving 50% of I_{max} (IC_{50}) to inhibit the synthesis (K_{in}) of the first platelet precursor compartment, as follows (IC, $F_{\text{Ini,Pre}} \cdot \text{Base}_{\text{Pre}}$):

$$\frac{d\text{Pre}_1}{dt} = \left(1 - \frac{I_{\text{max}} \cdot C_1}{IC_{50} + C_1}\right) \cdot \text{Stim}_{\text{Feedback}} \cdot K_{\text{in}} - k_{\text{tr}} \cdot \text{Pre}_1 \quad (6)$$

K_{in} is the zero-order rate of precursor synthesis, k_{tr} the first-order rate constant for transfer of platelet precursor cells, and Base_{Pre} the steady-state value for platelet precursors in the absence of drug, calculated as $\text{Base}_{\text{Pre}} = \text{Base}_{\text{PL}} \cdot k_{\text{out}}/k_{\text{tr}}$. The Base_{PL} is the baseline of platelets at steady state (i.e., without drug), and k_{out} the first-order rate constant for transfer of platelets. To account for a deviation of platelet precursor cells from their steady-state value at time zero, the factor $F_{\text{Ini,Pre}}$ was included. This factor accounts for patients who are not at the baseline of platelet precursor cells and platelets. The inclusion of the factors $F_{\text{Ini,Pre}}$ and $F_{\text{Ini,PL}}$ (see below) allowed the model to describe profiles with increasing or decreasing platelet counts during the first days of linezolid therapy.

The stimulation factor ($\text{Stim}_{\text{Feedback}}$) in equation 6 affected the synthesis of platelet precursor cells based on a function of the ratio of the baseline of the platelet count at steady state (Base_{PL}) and the current concentration of platelets in the circulation (PL; see below). The exponent (γ) was included to describe the extent of feedback, as described previously (12, 24). For a positive γ value, $\text{Stim}_{\text{Feedback}}$ is larger than 1 and therefore stimulates the synthesis of platelet precursors if PL decreases below Base_{PL}.

$$\text{Stim}_{\text{Feedback}} = \left(\frac{\text{Base}_{\text{PL}}}{\text{PL}}\right)^{\gamma} \quad (7)$$

If platelet counts increase above their steady-state value, the synthesis of platelet precursor cells is partially inhibited ($\text{Stim}_{\text{Feedback}} < 1$ if $\gamma > 0$). Newly generated platelet precursor cells (Pre_1) had to undergo transition through 15 transit compartments, reflecting their maturation time. The differential equation for the second to fifteenth ($i = 2$ to 15) platelet precursor compartments was as follows (IC, $F_{\text{Ini,Pre}} \cdot \text{Base}_{\text{Pre}}$):

$$\frac{d\text{Pre}_i}{dt} = k_{\text{tr}} \cdot \left(\text{Pre}_{i-1} - \text{Pre}_i\right) \quad (8)$$

The differential equations for the 15 platelet compartments were as follows (IC for both equations, $F_{\text{Ini,PL}} \cdot \text{Base}_{\text{PL}}$; $j = 2$ to 15):

$$\frac{d\text{PL}_1}{dt} = k_{\text{tr}} \cdot \text{Pre}_{15} - k_{\text{out}} \cdot \text{PL}_1 \quad (9)$$

$$\frac{d\text{PL}_j}{dt} = k_{\text{out}} \cdot \left(\text{PL}_{j-1} - \text{PL}_j\right) \quad (10)$$

To account for platelets not being at steady state at time zero, $F_{\text{Ini,PL}}$ was included as a factor with a fixed mean of 1 and an estimated between-subject variability (BSV) similar to $F_{\text{Ini,Pre}}$ for precursor cells (see equation 6). The output equation for the platelet count in the circulation (PL) was the average of the 15 platelet compartments, as follows:

$$\text{PL} = \frac{1}{15} \cdot \sum_1^{15} \text{PL}_j \quad (11)$$

Parameter variability and residual error model. The BSV was described by a log-normal distribution for all parameters (except I_{max}, which was modeled using a logistic transformation). Residual error was described by an additive plus proportional model for linezolid concentrations and platelets, as described previously (25, 26).

Covariate effect model. Body size was described by weight (WT), representing the lower value of ideal body weight (IBW) (27) and total body weight. A standard WT (WT_{STD}) of 65 kg was applied. The glomerular filtration rate (GFR) was estimated using the Cockcroft and Gault formula (28) for a patient with normal body size (WT_{STD} 65 kg) as described previously (29, 30). GFR_i for the ith patient with a nominal weight of 65 kg (age is in years, F_{Sex} is 0.85 for females and 1 for males, and SCR is the serum creatinine concentration in mg/dl) was calculated as follows:

$$\text{GFR}_i = \frac{140 - \text{age}_i}{\text{SCR}_i} \cdot \frac{65}{72} \cdot F_{\text{Sex},i} \quad (12)$$

The GFR was included as a time-dependent covariate; renal function (RF) was assumed to be linearly related to GFR and calculated by normalizing GFR_i to a standard GFR of 120 ml/min with $\text{RF}_i = \text{GFR}_i/\text{GFR}_{\text{STD}}$. The assumption on the correlation of renal function and creatinine clearance enabled the estimation of renal (CL_R) and nonrenal clearance (CL_{NR}) in the absence of urine data, as follows:

$$\text{CL} = F_{\text{Size,CL}} \cdot \left(\text{RF}_i \cdot \text{CL}_R + \text{CL}_{\text{NR}}\right) \quad (13)$$

$F_{\text{Size,CL}}$ is the allometric size factor for clearance using an allometric exponent of 0.75, and $F_{\text{Size,V}}$ is the allometric scale factor for volume of distribution with a fixed exponent of 1 and a reference WT of 65 kg (31).

Estimation. All parameters of the population PK/TD model were simultaneously estimated using the importance sampling algorithm (pmethod = 4) in parallelized S-ADAPT (version 1.57) via the SADAPT-TRAN facilitator (25, 26). Models were compared using the objective function ($-1 \cdot$ log-likelihood in S-ADAPT), plausibility of parameter estimates, standard diagnostic plots, visual predictive checks (VPCs) (32), and normalized prediction distribution error (NPDE) (33). Noncompartmental analysis using WinNonlin Pro (version 5.3) was performed to generate AUC_{24} values for the individual fitted concentration-time profiles that were predicted at 1,000 time points for each patient.

Simulations of platelet time courses for various linezolid dosage regimens. Monte Carlo simulations in 1,000 patients over 8 weeks (including 4 weeks of treatment and 4 weeks of recovery) for different oral dosage regimens were performed using Berkeley Madonna (version 8.3.18) to simulate the probability of reaching a nadir platelet count below 100×10^9/liter (threshold for clinically significant thrombocytopenia). The durations of therapy considered were 5, 7, 10, 14, and 28 days. The simulated patient population had a mean WT of 65 kg (coefficient of variation [CV], 18%) and a uniform distribution for creatinine clearance ranging from 15 to 125 ml/min. Simulations were performed for mean baseline platelet counts of 150, 250, and 400×10^9/liter. To consider small deviations of platelet and platelet precursor counts at initiation of therapy from baseline, the factors $F_{Ini,Pre}$ and $F_{Ini,PL}$ were applied in conjunction with their respective estimated BSV values.

Statistical analysis. Univariate analysis was carried out to identify risk factors for the development of thrombocytopenia (defined as a platelet count of $<100 \times 10^9$/liter). The variables evaluated (where available) included sex, age, weight, body mass index (BMI), baseline creatinine clearance, duration of linezolid administration, AUC_{24} during the first 7 days, Charlson's age-comorbidity score (34), comorbidities (diabetes, anemia, peripheral vascular disease, chronic obstructive pulmonary disease, liver disease, malignancy, gastrointentinal bleeding, and coagulopathy) and concomitant drug usage (heparin [including low-molecular-weight heparin], blood products, immunosuppressants, blood transfusion, and darbepoetin alpha). The Mann-Whitney test for quantitative variables and Fisher's exact test for qualitative variables were applied. The statistical program SPLUS version 8.2 was utilized for all analyses (SPLUS; Tibco).

RESULTS

Patient population. A total of 41 patients (25 male and 16 female) (Table 1) were included in the study (7 from the Alfred Hospital, 21 from the Austin Hospital, and 13 from UPMC). Patients were treated with linezolid (600 mg every 12 h [q12h]) for a mean duration of 22 days (standard deviation [SD], 15 days; range, 5 to 54 days). A total of 42 treatment courses were evaluated, as one patient from the UPMC was treated with linezolid on two separate occasions.

Population pharmacokinetics. A one-compartment disposition model with first-order elimination and three absorption lag compartments was chosen as the final PK model (Fig. 1; Table 2). The inclusion of 3 absorption lag compartments significantly improved the objective function ($P < 0.05$, likelihood ratio test) and provided improved curve fits compared to a one-compartment model with first-order absorption. The objective function was not improved by inclusion of a peripheral compartment or of saturable elimination, possibly due to the sparse nature of the data set (161 linezolid concentrations from 41 patients/42 treatment courses). The inclusion of creatinine clearance and weight as covariates reduced the variance in total clearance by 12% (from a CV of 52.2% to 48.9%).

The AUC_{24} during up to the first 7 days had an average of 223 mg · h/liter (CV, 52%), and the median (range) was 198 (65.2 to 551) mg · h/liter. The AUC_{24}/MIC values would have been above 100 in 90% of patients for a MIC of 1 mg/liter, in 50% of patients for a MIC of 2 mg/liter, and in 7% of patients for a MIC of 4 mg/liter.

Platelet data. There was high BSV in the observed baseline (mean, 288×10^9/liter; CV, 53.2%; range, 31.0 to 679×10^9/liter) and nadir (mean, 192×10^9/liter; CV, 71.1%; range, 13.0 to 598×10^9/liter) platelet counts, as well as in the maximal percent change of platelet counts during linezolid therapy (mean, 32.5%; CV, 102%; range, −79.2 to 91.0%). Fourteen patients (34%) developed severe

TABLE 1 Univariate evaluation of risk factors for development of thrombocytopenia

Characteristic	Value for patients who did or did not develop thrombocytopenia[a]		
	Yes ($n = 10$)	No ($n = 28$)	P value
Continuous variables [mean (CV%)]			
Age (yr)	54.0 (32.6)	60.5 (25.5)	0.50
Weight (kg)	73.1 (22.3)	75.1 (18.7)	0.60
Body mass index (kg/m²)	24.4 (16.5)	26.1 (16.4)	0.37
Baseline platelet count ($\times 10^9$/liter)	214 (37.2)	347 (41.2)	0.0084
Baseline creatinine clearance (ml/min/65 kg) (28)	68.3 (49.9)	71.2 (56.2)	1.00
Baseline serum albumin (g/liter)	31.1 (21.6)	26.5 (26.3)	0.075
Duration of linezolid treatment (days)	28.3 (63.7)	20.3 (62.1)	0.15
AUC_{24h} (mg · h/liter)	243 (50.3)	213 (54.0)	0.38
Charlson's age-comorbidity score (34)	4.70 (48.4)	5.14 (45.4)	0.43
Categorical variables [count (% within group)]			
Female	4 (40)	12 (43)	1.00
Diabetes	5 (50)	7 (25)	0.26
Anemia[b]	6 (60)	2 (7.1)	0.47
Peripheral vascular disease[b]	5 (50)	8 (29)	0.26
Liver disease[b]	3 (30)	8 (29)	1.00
Heparin	4 (40)	17 (61)	0.29
Blood transfusion	7 (70)	13 (46)	0.28
Immunosuppressants	5 (50)	9 (33)	0.45
Darbepoetin alpha	3 (30)	5 (18)	0.41

[a] Thrombocytopenia was defined as a platelet count of $<100 \times 10^9$/liter. Individuals with baseline counts of $<100 \times 10^9$/liter were removed ($n = 4$).
[b] Baseline comorbidity.

thrombocytopenia, defined as a platelet count of $<100 \times 10^9$/liter, of which 4 had platelet counts of $<100 \times 10^9$/liter at baseline. A total of 24 (57%) patients demonstrated ≥30% decreases from baseline to nadir.

Following removal of the 4 patients with baseline platelet counts of $<100 \times 10^9$/liter, baseline platelet count was the only variable identified to be associated with the occurrence of thrombocytopenia by univariate analysis ($P = 0.0084$) (Table 1).

Mechanism-based population PK/TD model. A delay between the initiation of linezolid therapy and the decline of platelets in most patients suggested that a precursor indirect response model would be more appropriate than a model without precursor compartments (35, 36). Models with 1, 3, 6, 9, 12, and 15 compartments each for precursor cells and platelets were evaluated. The objective function improved by a range of 4.4 to 86 with the inclusion of transit compartments, leading to the acceptance of a final model with 15 transit compartments each for precursor and platelet cells (Fig. 1). The objective function of a model with no precursors and only one platelet compartment was worse by 148 than that of the final model. The final model with 15 transit compartments also performed better than models with fewer transit compartments after inclusion of the feedback mechanism.

The platelet profiles for several patients suggested that platelet counts were not at steady state before the initiation of linezolid therapy, as shown for patients 1, 12, 28, 31, and 42 (Fig. 2). Overall, slightly over half of the patients showed a considerable increase or decrease of platelet count profiles during the first few days of

TABLE 2 Parameter estimates of the mechanism-based population pharmacokinetic/toxicodynamic model

Parameter	Symbol	Unit	Population mean (SE%)	BSV[a] (SE%)
Mean absorption lag time	T_{lag}[b]	Min	69.2 (16)	0.600 (47)
Absorption half-life	$T_{abs1/2}$[b]	Min	10.3 (6.3)	0.147 (83)
Total clearance	CL[c]	Liter/h	6.72	0.489 (24)
Nonrenal clearance	CL_{NR}[c]	Liter/h	4.55 (18)	
Renal clearance	CL_R[c]	Liter/h	2.17 (58)	
Volume of distribution	V[c]	Liter	44.3 (5.8)	0.036 (106)
Baseline of platelets	$Base_{PL}$	10^9/liter	252 (10)	0.651 (24)
Initial condition divided by individual steady-state estimate for platelet precursors	$F_{Ini,Pre}$		1 (fixed)[d]	0.215[d] (43)
Initial condition divided by individual steady-state estimate for platelets	$F_{Ini,PL}$		1 (fixed)[d]	0.236[d] (37)
Plasma linezolid concn resulting in 50% of maximal toxicity (I_{max} fixed to 1.0)	IC_{50}[e]	mg/liter	8.06[e] (35)	1.01 (60)
Mean life span of precursor cells	MTT_{Pre}[f]	Days	7.68 (11)	0.347 (34)
Mean life span of platelets	MTT_{PL}[f]	Days	6.80 (13)	0.203 (66)
Gamma, describing the extent of feedback	γ		1.02 (11)	0.15 (fixed)
Standard deviation of the additive residual error for plasma linezolid concentrations	SD_{in}	mg/liter	0.309 (56)	
Proportional residual error for plasma linezolid concentrations	SD_{sl}		0.225 (15)	
Standard deviation of the additive residual error for platelets	PD_{in}	10^9/liter	15.1 (19)	
Proportional residual error for platelets	PD_{sl}		0.0755 (17)	

[a] Between-subject variability (BSV) is expressed as the apparent coefficient of variation (i.e., the square root of the estimated variance). The estimate in parentheses (SE%) represents the relative standard error (i.e., the uncertainty of the estimate).
[b] k_{lag} was calculated as $3/T_{lag}$ and k_a as $Ln(2)/T_{abs1/2}$.
[c] Estimates for patients with a standard weight of 65 kg (as defined in the method section) and a standard creatinine clearance of 120 ml/min. If the volume of distribution and clearances were scaled using a standard body weight of 70 kg instead of 65 kg, the reported volume of distribution would be 7.69% and all clearances would be 5.72% higher than the values reported herein.
[d] The population means for $F_{Ini,Pre}$ and $F_{Ini,PL}$ were fixed to 1, and the associated BSV terms were estimated.
[e] A Hill coefficient and I_{max} were estimated, and both were close to 1.0 and eventually fixed to 1.0 for the final model. This choice had a minimal impact on the objective function.
[f] MTT, mean transit time. k_{tr} was calculated as $15/MTT_{Pre}$ and k_{out} as $15/MTT_{PL}$.

therapy. This clearly suggested that the inclusion of $F_{Ini,Pre}$ and $F_{Ini,PL}$ in the model was beneficial. Consistent with this, inclusion of the factors $F_{Ini,Pre}$ (estimated CV, 21.5%) and $F_{Ini,PL}$ (CV, 23.6%) improved the objective function by 76 ($P < 0.001$) (Table 2). These CVs suggested considerable deviations of the baseline precursor and baseline platelet counts from their steady-state value, which was considered in the Monte Carlo simulations.

Initially, models without a feedback mechanism were assessed. Inhibition of platelet precursor synthesis (mechanism 1) and direct killing of platelet precursor cells (mechanism 2) by linezolid yielded similar objective functions, whereas models with direct killing of platelets (mechanism 3) or stimulation of natural loss of platelets (k_{out}; mechanism 4) resulted in worsening of the objective functions by approximately 50 compared to models with mechanisms 1 and 2. For this reason, mechanisms 1 and 2 were chosen for further investigation as potential mechanisms of linezolid-induced thrombocytopenia.

Inclusion of the feedback mechanism affecting the synthesis of precursor cells improved the objective function by 99 ($P < 0.001$) for a model depicting inhibition of precursor synthesis (mechanism 1). A smaller improvement of 49 ($P < 0.001$) was seen after inclusion of feedback for the model with mechanism 2. Specifying the feedback as an accelerated transfer (k_{tr}) for platelet precursors did not significantly improve the objective function. Due to the best objective function for the model with mechanism 1, inhibition of precursor synthesis by linezolid and a feedback affecting the synthesis of precursor cells was chosen as the final model (Fig. 1). Inclusion of direct killing of platelets (mechanism 3) in addition to inhibition of synthesis of platelet precursors by linezolid (mechanism 1) yielded no improvement and a very slow maximal killing half-life of 35 days. Therefore, the final model included mechanism 1 but not mechanism 3.

The final PK/TD model yielded good individual curve fits for the complex time course of platelet counts (Fig. 2), including a lack of steady state at time zero and feedback. The IC_{50} was estimated as 8.06 mg/liter and had a large BSV with a CV of 101% (Table 2). Individual curve fits were precise and unbiased for plasma linezolid concentrations (slope, 1.04; r, 0.95) and platelets (slope, 1.01; r, 0.98) (Fig. 3). The population fits were reasonably unbiased and precise for plasma concentrations (slope, 1.10; r, 0.56). As expected, due to the large BSV in observed baseline platelet counts (observed CV of 52%), the population fits for platelets demonstrated no strong relationship (Fig. 3). After adjusting the population fits for the individual observed baseline platelet count, a moderate relationship emerged (slope, 1.08; r, 0.76) (Fig. 3). The NPDE plots for plasma concentrations (results not shown) and platelets (Fig. 3) were unbiased and reasonably mirrored a standard normal distribution.

The final mechanism-based model contained five estimated PK parameters and seven estimated PD parameters. The relative standard errors (SE%) were small (<20%) for all but two population means and slightly larger for these two parameters (Table 2). As expected, the SE% for the between-subject variability estimates were larger for our data set containing 42 plasma linezolid concentration and platelet profiles.

Simulation results. The predicted probability for nadir platelet counts below 100×10^9/liter was lowest for durations of therapy of 5 and 7 days and was substantially higher for 10, 14, and 28 days of therapy (Fig. 4). For a patient group with a simulated average baseline of 250×10^9/liter, 600 mg linezolid q12h for 10 or 14 days yielded noticeably higher toxicity than linezolid dosage regimens of 400 mg q12h or 600 mg q24h (Fig. 4A). In this patient group, front loading of 1,200 mg q12h or of 2,400 mg q12h yielded levels of toxicity similar to those yielded by 600 mg q12h, if the
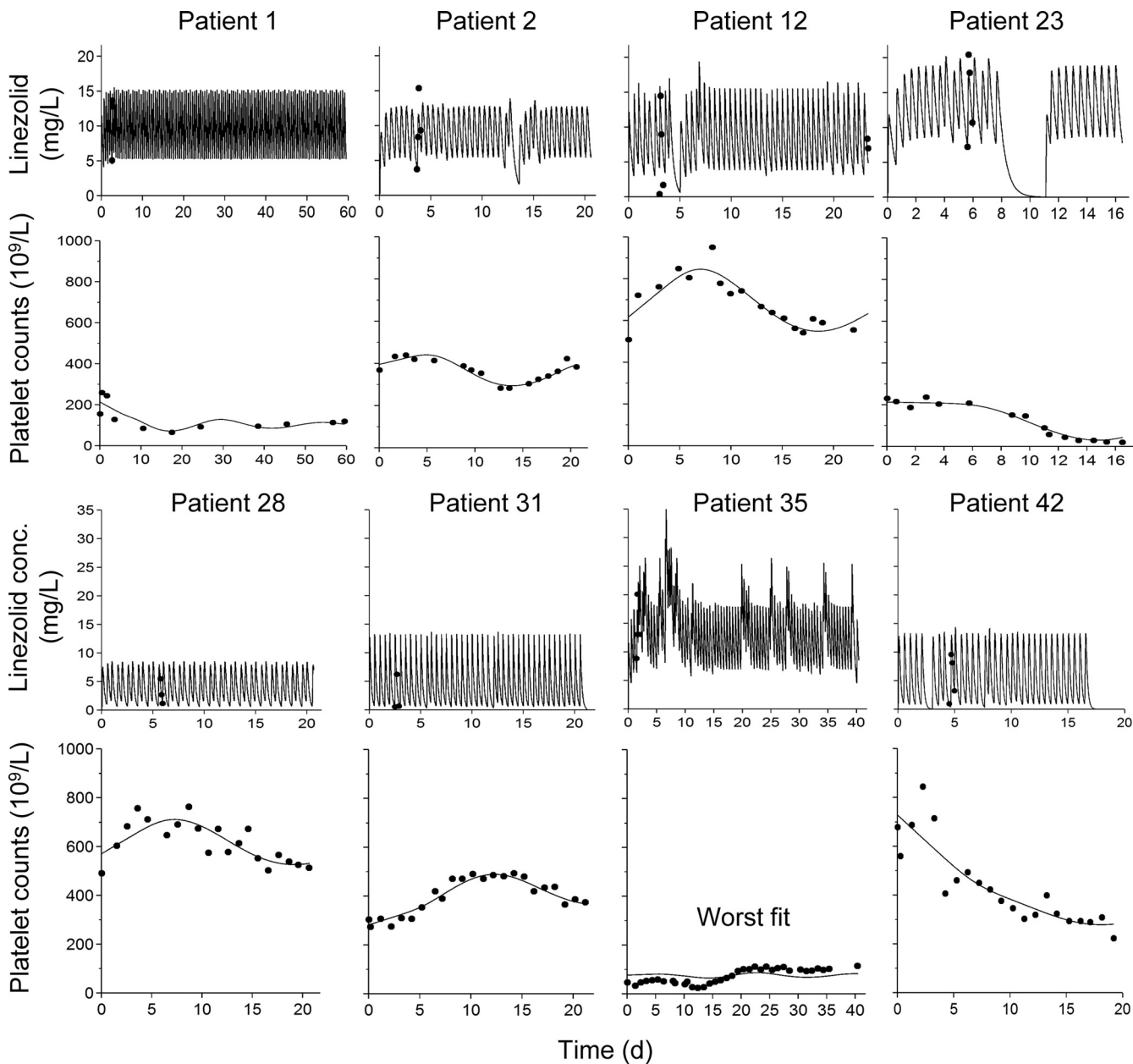
FIG 2 Observed (dots) and individual fitted (lines) plasma linezolid concentrations and platelet counts for a representative selection of patients. Note that the platelet profiles for patients 12, 28, and 31 were rising during the first week and therefore did not start at steady state.

front loading was constrained to two dosing intervals over the first day of therapy (Fig. 4B).

As expected for a population with a mean baseline platelet count of 150×10^9/liter, significantly more toxicity was predicted for all regimens (Fig. 4C). Considerably less toxicity was predicted for a patient population with a mean baseline of 400×10^9/liter. At this higher baseline, front loading of 1,200 mg q12h for 5 days followed by 300 mg or 600 mg q12h yielded a toxicity comparable to that of the standard 600 mg q12h regimen (Fig. 4D).

DISCUSSION

The relationship between linezolid PK and TD was first examined in a study of a highly debilitated, critically ill compassionate-use

population (10, 37, 38) and was further investigated in this study with a patient population more typical of postapproval usage patterns. Mechanism-based modeling was performed to explore potential mechanisms of linezolid toxicity and to describe and predict platelet counts over time for standard and PD-optimized linezolid dosage regimens with different durations of therapy. The modeling analysis by Sasaki et al. (12) for Japanese patients reported a considerably increased risk of toxicity for common linezolid dosage regimens in patients with impaired renal function or severe liver cirrhosis.

In the current study, patients were treated with linezolid for a wide range of infecting organisms, infection types, and therapy durations (5 to 54 days; mean, 22 days). Treatment extended be-
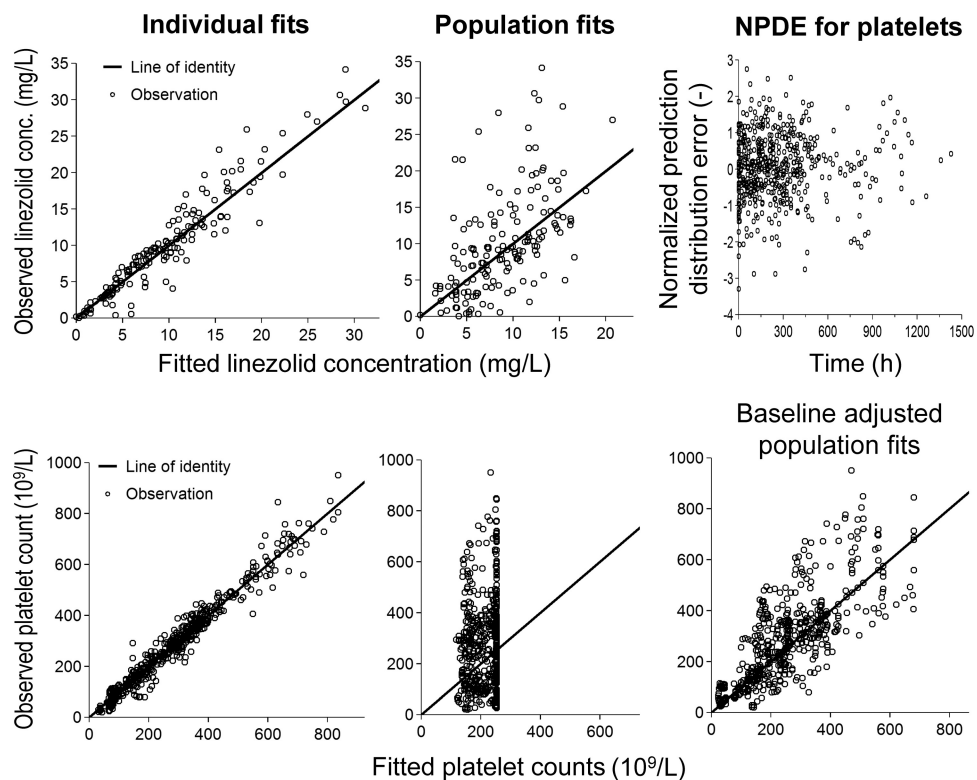
FIG 3 Observations versus individual (left) and population-fitted (middle) plots for linezolid concentrations in plasma (top) and platelet counts (bottom). The right-hand pair of plots show normalized prediction distribution errors (NPDE) for platelets and the baseline-adjusted population fit plot. For baseline adjustment, the population-fitted profiles were multiplied by the ratio of the individual observed baseline at time zero for the respective patient and the population mean baseline.

yond the maximum recommended duration of 28 days in eight patients (1). The high BSV in PK in the current study was consistent with that reported in other patient populations (18, 37) and has both potential efficacy and toxicity implications. The population pharmacodynamic model for the compassionate-use population (38) linked AUC/MIC values of >100 to clinical cure and bacterial eradication endpoints. In the present study, 50% of patients would have failed to reach the reported target AUC/MIC exposure of 100 (38) based on a MIC$_{90}$ of 2 mg/liter for linezolid (39).

A one-compartment population PK model with first-order elimination and an oral absorption lag best described the current data. Our final PK model was linear and thus differed from that for the compassionate-use population data, which included parallel linear renal clearance and Michaelis-Menten nonrenal clearance pathways (37). The sparsely sampled plasma linezolid concentrations and relatively small sample size of the current study potentially contributed to these differences. In agreement with the model by Meagher et al. (37), creatinine clearance explained some of the variability of total clearance.

Approximately one third of patients in the current study developed thrombocytopenia, defined as platelet counts of less than 100 × 10^9/liter, consistent with reports on postapproval use (6, 7, 12). Baseline platelet count was the only variable significantly associated with the occurrence of thrombocytopenia based on univariate analysis. The small number of observed associations limited further exploration of risk factors via multivariate analysis.

This was potentially caused by our relatively small sample size and other clinical factors in our patient group.

Several previously proposed mechanisms for linezolid-induced thrombocytopenia (13–15) were used to guide our modeling analysis. Sasaki et al. (12) described the toxicity of linezolid on platelets by a mechanism-based model with one progenitor pool compartment, three transit compartments, and one compartment for circulating platelets. This model was originally developed for the effect of anticancer drugs on neutrophils and leukocytes (24) and assumes a linear inhibition of synthesis of progenitor cells and a monoexponential function (i.e., one compartment) for circulating platelets.

As shown by prior studies (22, 23), the life span distribution of circulating platelets is, however, complex and, as such, not likely to be well described by either a monoexponential process or a single life span for all platelets. Therefore, we evaluated different shapes for the life span distribution for platelets and precursor cells by exploring models with different numbers of transit compartments. As indicated by the final model with 15 transit compartments, the modeled distribution of life spans for platelets and platelet precursor cells was narrower than that predicted by a monoexponential function discussed previously (20, 40). The estimated mean transit times of 7.68 days (CV, 34.7%) for precursor cells and 6.80 days (20.3%) for platelets (Table 2) were in excellent agreement with estimates in the literature for the maturation (approximately 9 days) and life span of platelets (5 to 10 days) (21–23).
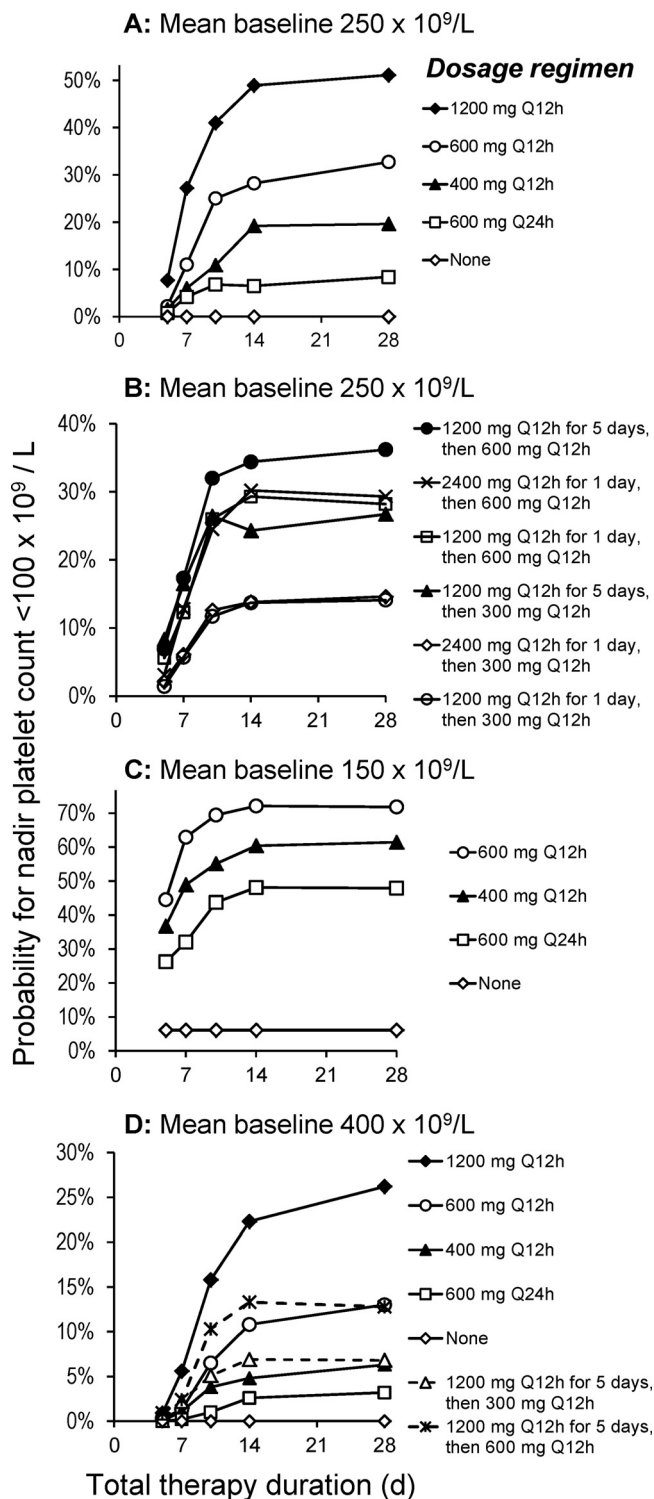
FIG 4 Simulated probabilities for nadir platelet counts below 100×10^9/liter for various normal and front-loaded linezolid dosage regimens when mean baselines were as indicated.

The final model described the linezolid-induced thrombocytopenia by an inhibition of the synthesis of platelet precursor cells by linezolid. The inclusion of a feedback mechanism with a lack of platelets stimulating the production of platelet precursor cells

(Fig. 1) improved the model fits significantly. The estimated exponent (γ) of 1.02 indicated a stronger feedback than was estimated by Sasaki et al. (0.203) (12). To further investigate this feedback, the model structure of Sasaki et al. was applied to the current data set and yielded an exponent of 2.3, suggesting an even stronger feedback than was estimated by the present model (Table 2). While the reasons for these different extents of feedback are not fully understood, our additional analysis shows that this may be partly attributed to the different data sets used, and feedback was clearly beneficial.

If platelets decline below their steady-state baseline, the feedback upregulates the synthesis of platelet precursor cells for the duration of linezolid therapy. Therefore, the model predicts that the lowest platelet count usually occurs after 2 to 3 weeks of linezolid therapy, if the linezolid exposure is constant during therapy. This feature was consistent with our data set (see the data for patients 2 and 23 in Fig. 2, for example).

The proposed mechanism-based model (Fig. 1) contained 12 structural model parameters which were estimated with good precision (SE% of <20% for all but two population means). As expected, the uncertainty of the estimated BSV parameters was larger. However, the NPDE (Fig. 3) suggested that the variability between patients was well captured by our model and BSV parameter estimates. While our study only contained 42 plasma linezolid concentration and platelet profiles, these results suggested that our sample size and study design were adequate to support the proposed mechanism-based model (Table 2). This is in agreement with a previous simulation-estimation study using a much more complex PK/PD model with 45 structural model parameters that were simultaneously estimated based on data from 48 patients using a sparse sampling design (26).

Our Monte Carlo simulations predicted a substantially lower risk for nadir platelet counts of below 100×10^9/liter for therapy durations of 5 to 7 days than for durations of 10 to 28 days (Fig. 4). This prediction was in good agreement with the observed probability of thrombocytopenia in the study by Nukui et al. (41) and with the reported higher incidence of thrombocytopenia development after 14 days of treatment (2, 5). While the predicted probability for platelet toxicity did not differ noticeably for therapy durations of 14 or 28 days, this prediction may be affected by a time-dependent autoinhibition of linezolid clearance (not included in the current model). The latter model feature was previously reported based on data from healthy volunteers (18, 42). Overall, therapy duration was a more important predictor of toxicity than was linezolid dose.

As expected, a higher risk for toxicity was predicted for a low baseline platelet count of 150×10^9/liter than for baseline counts of 250×10^9/liter or 400×10^9/liter. Therefore, high-dose linezolid regimens seem not warranted for patients with low baseline platelet counts. Front-loaded linezolid regimens have recently demonstrated promising bactericidal activity (43, 44). Based on the predicted toxicity for patients with normal to high baseline platelet counts (Fig. 4), more aggressive, PD-optimized dosing of 1,200 mg linezolid q12h for up to 5 days followed by 600 (or 300) mg q12h may have utility in patients with baseline platelet counts of 400×10^9/liter or above.

In summary, baseline platelet counts and therapy durations of 10 days or longer were the most important predictors of linezolid toxicity. Even at relatively high linezolid doses, therapy for 5 to 7 days was predicted to be substantially safer than longer treatment

durations. For patients with normal and high baseline platelet counts, innovative, PD-optimized, front-loaded dosage regimens were predicted to be at least as safe as a standard regimen of 600 mg every 12 h. Inhibition of synthesis of platelet precursor cells was identified as the most likely mechanism of toxicity. The mechanism-based model developed can be used to individualize linezolid therapy to maximize the efficacy and minimize the risk for toxicity. In view of the demonstrated increased risk of toxicity observed after 2 weeks of linezolid therapy and large variability in PK and TD, close monitoring of patients for development of toxicity remains important.

ACKNOWLEDGMENTS

REFERENCES

1. **Wilcox MH.** 2003. Efficacy of linezolid versus comparator therapies in Gram-positive infections. J. Antimicrob. Chemother. **51**(Suppl 2)**:**ii27–ii35. http://dx.doi.org/10.1093/jac/dkg251.

2. **Birmingham MC, Rayner CR, Meagher AK, Flavin SM, Batts DH, Schentag JJ.** 2003. Linezolid for the treatment of multidrug-resistant, gram-positive infections: experience from a compassionate-use program. Clin. Infect. Dis. **36**:159–168. http://dx.doi.org/10.1086/345744.

3. **Welshman IR, Sisson TA, Jungbluth GL, Stalker DJ, Hopkins NK.** 2001. Linezolid absolute bioavailability and the effect of food on oral bioavailability. Biopharm. Drug Dispos. **22**:91–97. http://dx.doi.org/10.1002/bdd.255.

4. **Stalker DJ, Jungbluth GL, Hopkins NK, Batts DH.** 2003. Pharmacokinetics and tolerance of single- and multiple-dose oral or intravenous linezolid, an oxazolidinone antibiotic, in healthy volunteers. J. Antimicrob. Chemother. **51**:1239–1246. http://dx.doi.org/10.1093/jac/dkg180.

5. **Rubinstein E, Isturiz R, Standiford HC, Smith LG, Oliphant TH, Cammarata S, Hafkin B, Le V, Remington J.** 2003. Worldwide assessment of linezolid's clinical safety and tolerability: comparator-controlled phase III studies. Antimicrob. Agents Chemother. **47**:1824–1831. http://dx.doi.org/10.1128/AAC.47.6.1824-1831.2003.

6. **Attassi K, Hershberger E, Alam R, Zervos MJ.** 2002. Thrombocytopenia associated with linezolid therapy. Clin. Infect. Dis. **34**:695–698. http://dx.doi.org/10.1086/338403.

7. **Orrick JJ, Johns T, Janelle J, Ramphal R.** 2002. Thrombocytopenia secondary to linezolid administration: what is the risk? Clin. Infect. Dis. **35**:348–349. http://dx.doi.org/10.1086/341310.

8. **Grau S, Morales-Molina JA, Mateu-de Antonio J, Marin-Casino M, Alvarez-Lerma F.** 2005. Linezolid: low pre-treatment platelet values could increase the risk of thrombocytopenia. J. Antimicrob. Chemother. **56**:440–441. http://dx.doi.org/10.1093/jac/dki202.

9. **Matsumoto K, Takeshita A, Ikawa K, Shigemi A, Yaji K, Shimodozono Y, Morikawa N, Takeda Y, Yamada K.** 2010. Higher linezolid exposure and higher frequency of thrombocytopenia in patients with renal dysfunction. Int. J. Antimicrob. Agents **36**:179–181. http://dx.doi.org/10.1016/j.ijantimicag.2010.02.019.

10. **Bishop E, Melvani S, Howden BP, Charles PG, Grayson ML.** 2006. Good clinical outcomes but high rates of adverse reactions during linezolid therapy for serious infections: a proposed protocol for monitoring therapy in complex patients. Antimicrob. Agents Chemother. **50**:1599–1602. http://dx.doi.org/10.1128/AAC.50.4.1599-1602.2006.

11. **Forrest A, Rayner CR, Meager AK, Birmingham MC, Schentag JJ.** 2000. Pharmacostatistical modelling of hematologic effects of linezolid in seriously-ill patients, abstr 283. Abstr. 44th Intersci. Conf. Antimicrob. Agents Chemother. American Society for Microbiology, Washington, DC.

12. **Sasaki T, Takane H, Ogawa K, Isagawa S, Hirota T, Higuchi S, Horii T, Otsubo K, Ieiri I.** 2011. Population pharmacokinetic and pharmacodynamic analysis of linezolid and a hematologic side effect, thrombocytopenia, in Japanese patients. Antimicrob. Agents Chemother. **55**:1867–1873. http://dx.doi.org/10.1128/AAC.01185-10.

13. **Green SL, Maddox JC, Huttenbach ED.** 2001. Linezolid and reversible myelosuppression. JAMA **285**:1291. http://dx.doi.org/10.1001/jama.285.10.1291.

14. **Bernstein WB, Trotta RF, Rector JT, Tjaden JA, Barile AJ.** 2003. Mechanisms for linezolid-induced anemia and thrombocytopenia. Ann. Pharmacother. **37**:517–520. http://dx.doi.org/10.1345/aph.1C361.

15. **Pascoalinho D, Vilas MJ, Coelho L, Moreira P.** 2011. Linezolid-related immune-mediated severe thrombocytopenia. Int. J. Antimicrob. Agents **37**:88–89. http://dx.doi.org/10.1016/j.ijantimicag.2010.10.001.

16. **Boak LM, Li J, Nation RL, Rayner CR.** 2006. High-performance liquid chromatographic method for simple and rapid determination of linezolid in human plasma. Biomed. Chromatogr. **20**:782–786. http://dx.doi.org/10.1002/bmc.597.

17. **Gordi T, Xie R, Huong NV, Huong DX, Karlsson MO, Ashton M.** 2005. A semiphysiological pharmacokinetic model for artemisinin in healthy subjects incorporating autoinduction of metabolism and saturable first-pass hepatic extraction. Br. J. Clin. Pharmacol. **59**:189–198. http://dx.doi.org/10.1111/j.1365-2125.2004.02321.x.

18. **Plock N, Buerger C, Joukhadar C, Kljucar S, Kloft C.** 2007. Does linezolid inhibit its own metabolism? Population pharmacokinetics as a tool to explain the observed nonlinearity in both healthy volunteers and septic patients. Drug Metab. Dispos. **35**:1816–1823. http://dx.doi.org/10.1124/dmd.106.013755.

19. **Bulitta JB, Okusanya OO, Forrest A, Bhavnani SM, Clark K, Still JG, Fernandes P, Ambrose PG.** 2013. Population pharmacokinetics of fusidic acid: rationale for front-loaded dosing regimens due to autoinhibition of clearance. Antimicrob. Agents Chemother. **57**:498–507. http://dx.doi.org/10.1128/AAC.01354-12.

20. **Krzyzanski W.** 2011. Interpretation of transit compartments pharmacodynamic models as lifespan based indirect response models. J. Pharmacokinet. Pharmacodyn. **38**:179–204. http://dx.doi.org/10.1007/s10928-010-9183-z.

21. **Muller U, Kulinna J, Luber J, Hebestreit HP, Mayer M, Kempgens U, Queisser W.** 1977. In vivo study of platelet kinetics by 75Se-methionine in different haematological disorders. Blut **34**:31–38. http://dx.doi.org/10.1007/BF00997036.

22. **Najean Y, Ardaillou N, Dresch C.** 1969. Platelet lifespan. Annu. Rev. Med. **20**:47–62. http://dx.doi.org/10.1146/annurev.me.20.020169.000403.

23. **Shulman NR, Jordan JV, Jr, Falchuk S.** 1985. A normal fixed-loss component of platelet utilization accounting for short survival of transfused platelets. Ann. N. Y. Acad. Sci. **459**:367–374. http://dx.doi.org/10.1111/j.1749-6632.1985.tb20846.x.

24. **Friberg LE, Karlsson MO.** 2003. Mechanistic models for myelosuppression. Invest. New Drugs **21**:183–194. http://dx.doi.org/10.1023/A:1023573429626.

25. **Bulitta JB, Bingolbali A, Shin BS, Landersdorfer CB.** 2011. Development of a new pre- and post-processing tool (SADAPT-TRAN) for nonlinear mixed-effects modeling in S-ADAPT. AAPS J. **13**:201–211. http://dx.doi.org/10.1208/s12248-011-9257-x.

26. **Bulitta JB, Landersdorfer CB.** 2011. Performance and robustness of the Monte Carlo importance sampling algorithm using parallelized S-ADAPT for basic and complex mechanistic models. AAPS J. **13**:212–226. http://dx.doi.org/10.1208/s12248-011-9258-9.

27. **Devine BJ.** 1974. Case number 25: gentamicin therapy. Drug Intell. Clin. Pharm. **8**:650–655.

28. **Cockcroft DW, Gault MH.** 1976. Prediction of creatinine clearance from serum creatinine. Nephron **16**:31–41. http://dx.doi.org/10.1159/000180580.

29. **Matthews I, Kirkpatrick C, Holford N.** 2004. Quantitative justification for target concentration intervention—parameter variability and predictive performance using population pharmacokinetic models for aminoglycosides. Br. J. Clin. Pharmacol. **58**:8–19. http://dx.doi.org/10.1111/j.1365-2125.2004.02114.x.

30. **Bulitta JB, Duffull SB, Landersdorfer CB, Kinzig M, Holzgrabe U, Stephan U, Drusano GL, Sorgel F.** 2009. Comparison of the pharmacokinetics and pharmacodynamic profile of carumonam in cystic fibrosis patients and healthy volunteers. Diagn. Microbiol. Infect. Dis. **65**:130–141. http://dx.doi.org/10.1016/j.diagmicrobio.2009.06.018.

31. **Anderson BJ, Holford NH.** 2008. Mechanism-based concepts of size and maturity in pharmacokinetics. Annu. Rev. Pharmacol. Toxicol. **48**:303–332. http://dx.doi.org/10.1146/annurev.pharmtox.48.113006.094708.

32. **Bulitta JB, Duffull SB, Kinzig-Schippers M, Holzgrabe U, Stephan U, Drusano GL, Sorgel F.** 2007. Systematic comparison of the population pharmacokinetics and pharmacodynamics of piperacillin in cystic fibrosis patients and healthy volunteers. Antimicrob. Agents Chemother. **51:** 2497–2507. http://dx.doi.org/10.1128/AAC.01477-06.

33. **Brendel K, Comets E, Laffont C, Laveille C, Mentre F.** 2006. Metrics for external model evaluation with an application to the population pharmacokinetics of gliclazide. Pharm. Res. **23:**2036–2049. http://dx.doi.org/10.1007/s11095-006-9067-5.

34. **Charlson M, Szatrowski TP, Peterson J, Gold J.** 1994. Validation of a combined comorbidity index. J. Clin. Epidemiol. **47:**1245–1251. http://dx.doi.org/10.1016/0895-4356(94)90129-5.

35. **Dayneka NL, Garg V, Jusko WJ.** 1993. Comparison of four basic models of indirect pharmacodynamic responses. J. Pharmacokinet. Biopharm. **21:**457–478. http://dx.doi.org/10.1007/BF01061691.

36. **Sharma A, Slugg PH, Hammett JL, Jusko WJ.** 1998. Estimation of oral bioavailability of a long half-life drug in healthy subjects. Pharm. Res. **15:**1782–1786. http://dx.doi.org/10.1023/A:1011977116543.

37. **Meagher AK, Forrest A, Rayner CR, Birmingham MC, Schentag JJ.** 2003. Population pharmacokinetics of linezolid in patients treated in a compassionate-use program. Antimicrob. Agents Chemother. **47:**548–553. http://dx.doi.org/10.1128/AAC.47.2.548-553.2003.

38. **Rayner CR, Forrest A, Meagher AK, Birmingham MC, Schentag JJ.** 2003. Clinical pharmacodynamics of linezolid in seriously ill patients treated in a compassionate use programme. Clin. Pharmacokinet. **42:** 1411–1423. http://dx.doi.org/10.2165/00003088-200342150-00007.

39. **Draghi DC, Sheehan DJ, Hogan P, Sahm DF.** 2005. In vitro activity of linezolid against key gram-positive organisms isolated in the United States: results of the LEADER 2004 surveillance program. Antimicrob. Agents Chemother. **49:**5024–5032. http://dx.doi.org/10.1128/AAC.49.12.5024-5032.2005.

40. **Bulitta JB, Zhao P, Arnold RD, Kessler DR, Daifuku R, Pratt J, Luciano G, Hanauske AR, Gelderblom H, Awada A, Jusko WJ.** 2009. Multiple-pool cell lifespan models for neutropenia to assess the population pharmacodynamics of unbound paclitaxel from two formulations in cancer patients. Cancer Chemother. Pharmacol. **63:**1035–1048. http://dx.doi.org/10.1007/s00280-008-0828-1.

41. **Nukui Y, Hatakeyama S, Okamoto K, Yamamoto T, Hisaka A, Suzuki H, Yata N, Yotsuyanagi H, Moriya K.** 2013. High plasma linezolid concentration and impaired renal function affect development of linezolid-induced thrombocytopenia. J. Antimicrob. Chemother. **68:**2128–2133. http://dx.doi.org/10.1093/jac/dkt133.

42. **Bhalodi AA, Papasavas PK, Tishler DS, Nicolau DP, Kuti JL.** 2013. Pharmacokinetics of intravenous linezolid in moderately to morbidly obese adults. Antimicrob. Agents Chemother. **57:**1144–1149. http://dx.doi.org/10.1128/AAC.01453-12.

43. **Tsuji B, Brown T, Parasrampuria R, Brazeau DA, Forrest A, Kelchlin PA, Holden PN, Peloquin CA, Hanna D, Bulitta JB.** 2012. Front-loaded linezolid regimens result in increased killing and suppression of the accessory gene regulator system of Staphylococcus aureus. Antimicrob. Agents Chemother. **56:**3712–3719. http://dx.doi.org/10.1128/AAC.05453-11.

44. **Tsuji BT, Bulitta JB, Brown T, Forrest A, Kelchlin PA, Holden PN, Peloquin CA, Skerlos L, Hanna D.** 2012. Pharmacodynamics of early, high-dose linezolid against vancomycin-resistant enterococci with elevated MICs and pre-existing genetic mutations. J. Antimicrob. Chemother. **67:**2182–2190. http://dx.doi.org/10.1093/jac/dks201.